Quantum Inf Process (2016) 15:2359–2376
DOI 10.1007/s11128-016-1284-1

Fast generation of N-atom Greenberger–Horne–Zeilinger state in separate coupled cavities via transitionless quantum driving

Wu-Jiang Shan[1] · Yan Xia[1] · Ye-Hong Chen[1] · Jie Song[2]

Received: 17 July 2015 / Accepted: 22 February 2016 / Published online: 15 March 2016

Abstract By jointly using quantum Zeno dynamics and the approach of "transitionless quantum driving (TQD)" proposed by Berry to construct shortcuts to adiabatic passage, we propose an efficient scheme to fast generate multiatom Greenberger–Horne–Zeilinger (GHZ) state in separate cavities connected by optical fibers only by one-step manipulation. We first detail the generation of the three-atom GHZ state via TQD; then, we compare the proposed TQD scheme with the traditional ones with adiabatic passage. At last, the influence of various decoherence factors, such as spontaneous emission, cavity decay and fiber photon leakage, is discussed by numerical simulations. All of the results show that the present TQD scheme is fast and insensitive to atomic spontaneous emission and fiber photon leakage. Furthermore, the scheme can be directly generalized to realize N-atom GHZ state generation by the same principle in theory.

Keywords Quantum Zeno dynamics · Transitionless quantum driving · Greenberger–Horne–Zeilinger state · Cavity quantum electrodynamics

1 Introduction

Quantum entanglement is not only one of the most important features in quantum mechanics [1,2], but also a key resource for testing quantum mechanics against local

✉ Yan Xia
xia-208@163.com

Jie Song
jsong@hit.edu.cn

1 Department of Physics, Fuzhou University, Fuzhou 350002, China

2 Department of Physics, Harbin Institute of Technology, Harbin 150001, China

hidden theory [3]. Recently, the entangled states have attracted considerable attention because of their fundamental scientific significance [4] and have been applied in many fields in quantum information processing (QIP), such as quantum computing [5], quantum cryptography [6], quantum teleportation [7,8] and quantum secret sharing [9]. These promising applications have greatly motivated the researches in the generation of entangled states.

It is worth noting that a typical entangled state so-called Greenberger–Horne–Zeilinger (GHZ) state $|\mathrm{GHZ}\rangle = \frac{1}{\sqrt{2}}(|000\rangle + |111\rangle)$, first proposed and named by Greenberger et al. [10], has raised much interest. Contrary to other entangled states, the GHZ state exhibits some special features, such as it is the maximally entangled state and can maximally violate the Bell inequalities [12]. In 2001, Zheng has proposed a scheme to test quantum mechanics against local hidden theory without the Bell's inequalities by use of multiatom GHZ state [13]. Therefore, great interest has arisen regarding the significant role of GHZ state in the foundations of quantum mechanics measurement theory and quantum communication. At present, the first and main problem we face is how to fast and efficiently generate GHZ state by using current technologies. To our knowledge, in some experimental systems, such as trapped ions systems [14], photons systems [15,16], and atoms systems [17], scientists have realized the generation of such GHZ state. Recently, a promising experimental instrument named cavity quantum electrodynamics (C-QED), which concerns the interaction between the atom and the quantized field within cavity [18], has aroused much attention. Based on C-QED, many theoretical schemes for generating GHZ state have been proposed. For example, Li et al. [19] have proposed a scheme to generate multiatom GHZ state under the resonant condition by Zeno dynamics, but the scheme is sensitive to the atomic spontaneous emission and fiber photonic leakage. Hao et al. [20] have proposed an efficient scheme to generate multiatom GHZ state under the resonant condition via adiabatic passage, but it takes too long time. Chen et al. have proposed a smart scheme to overcome the above drawbacks, but the scheme needs to trap three atoms in one cavity [21], such design is difficult to manipulate each atom in experiment and to construct a large-scale quantum network.

On the other hand, in modern quantum application field, an important method to manipulate the states of a quantum system, is adiabatic passage, included "rapid" adiabatic passage (RAP), stimulated Raman adiabatic passage (STIRAP), and their variants [22]. The adiabatic passage covers the shortage with respect to errors or fluctuations of the parameters compared with the resonant pulses, but its evolution speed is very slow, so it may be useless in some cases. In recent years, shortcuts to adiabatic passage (STAP), which accelerates a slow adiabatic quantum process via a non-adiabatic route, has aroused a great deal of attention. Many theoretical proposals have been presented to realize QIP, such as fast population transfer [23–26], fast entanglement generation [25,27], and fast implementation of quantum phase gates [28,29]. To our knowledge, the main methods to construct effective shortcuts have two forms: one is invariant-based inverse engineering-based Lewis–Riesenfeld invariant (IBLR) [30] and the other is transitionless quantum driving (TQD) [31], which is pointed out by Berry. The two methods are strongly related [32], but also have their own characteristics. For example, the former does not need to modify the

original Hamiltonian $H_0(t)$, but the algorithm is suitable for some special physical models. The latter needs to modify the original Hamiltonian $H_0(t)$ to the "counter-diabatic driving" (CDD) Hamiltonian $H(t)$ to speed up the quantum process. The fixed Hamiltonian $H(t)$ can be obtained in theory, but it does not usually exist in real experiment.

In addition, the quantum Zeno effect (QZE), first understood by Neumann [33] and named by Misra and Sudarshan [34], exhibits a especially experimental phenomenon that transitions between quantum states can be hindered by frequent measurement. The system will evolve away from its initial state and remain in the so-called Zeno subspace defined by the measure due to frequently projecting onto a multidimensional subspace [35,36]. This is so-called quantum Zeno dynamics (QZD). Without making using of projection operators and non-unitary, "a continuous coupling" can obtain the same quantum Zeno effect instead of discontinuous measurements [37,38]. Now, we give a brief introduction of the quantum Zeno dynamics in the form of continuous coupling [38]. Suppose that the system and its continuously coupling external system are governed by the total Hamiltonian $H_{\text{tot}} = H_s + KH_e$, where H_s is the Hamiltonian of the quantum system to be investigated, H_e is an additional Hamiltonian caused by the interaction with the external system, K is the coupling constant. In the limit $K \to \infty$, the evolution operator of system can be expressed as $U(t) = \exp[-it\sum_n (K\eta_n P_n + P_n H_s P_n)]$, where P_n is the eigenprojection of H_e corresponding to the eigenvalue η_n, i.e., $H_e P_n = \eta_n P_n$ [39].

Inspired by the above useful works, we make use of Zeno dynamics and TQD to construct STAP to generate N-atom GHZ state in C-QED. Our scheme has the following advantages: (1) The atoms are trapped in different cavities so that the single-qubit manipulation is more available in experiment. (2) The fast quantum entangled state generation for multiparticle in spatially separated atoms can be achieved in one step. (3) Numerical results show that our scheme is not only fast, but also robust against variations in the experimental parameters and decoherence caused by atomic spontaneous emission and fiber photon leakage. In fact, further research shows that the total operation time for the scheme is irrelevant to the number N of qubits.

The paper is organized as follows. In Sect. 2, we give a brief introduction to the approach of TQD proposed by Berry. In Sect. 3, we introduce the physical modal and the systematic approximation by QZD. In Sect. 4, we propose the scheme to generate the three-atom GHZ state via TQD and adiabatic passage, respectively. The decoherence caused by various factors is discussed by the numerical simulation. In Sect. 5, we directly generalize the scheme in Sect. 4 to generate N-atom GHZ state in one step. At last, we discuss the experimental feasibility and make a conclusion about the scheme in Sect. 6.

2 Transitionless quantum driving

Suppose a system is dominated by a time-dependent Hamiltonian $H_o(t)$ with instantaneous eigenvectors $|\phi_n(t)\rangle$ and eigenvalues $E_n(t)$,

$$H_o(t)|\phi_n(t)\rangle = E_n(t)|\phi_n(t)\rangle. \tag{1}$$

When a slow change satisfying the adiabatic condition happens, the system governed by $H_o(t)$ can be expressed at time t

$$|\psi(t)\rangle = e^{i\xi_n(t)}|\phi_n(t)\rangle,$$
$$\xi_n(t) = -\frac{1}{h}\int_0^t \mathrm{d}t' E_n(t') + i\int_0^t \mathrm{d}t'\langle\phi_n(t')|\partial_{t'}\phi_n(t')\rangle, \tag{2}$$

where $\partial_{t'} = \frac{\partial}{\partial_{t'}}$. Because the instantaneous eigenstates $|\phi_n(t)\rangle$ do not meet the Schrödinger equation, i.e., $i\hbar\partial_t|\phi_n(t)\rangle \neq H_0|\phi_n(t)\rangle$, a finite probability that the system is in the state $|\phi_{m\neq n}(t)\rangle$ will occur during the whole evolution process even under the adiabatic condition.

To construct the Hamiltonian $H(t)$ that drives the instantaneous eigenvector $|\phi_n(t)\rangle$ exactly, i.e., there are no transitions between different eigenvectors during the whole evolution process, we define the unitary operator

$$U = \sum_n e^{i\xi_n(t)}|\phi_n(t)\rangle\langle\phi_n(0)|, \tag{3}$$

we can formally solve the Schrödinger equation

$$H(t) = i\hbar(\partial_t U)U^\dagger. \tag{4}$$

Substituting Eq. (3) into Eq. (4), the Hamiltonian $H(t)$ can be expressed

$$H(t) = i\hbar\sum_n\left(|\partial_t\phi_n\rangle\langle\phi_n| - \hbar\sum_n|\phi_n\rangle\dot{\xi}_n\langle\phi_n|\right), \tag{5}$$

the simplest choice is $E_n = 0$, for which the bare states $|\phi_n(t)\rangle$, with no phase factors, are driven by

$$H(t) = i\hbar\sum_n|\partial_t\phi_n\rangle\langle\phi_n|. \tag{6}$$

3 Physical modal and systematic approximation by QZD

For the sake of the clearness, let us first consider the physical modal that three identical atoms a_1, a_2 and a_3 are trapped in three linearly arranged optical cavities C_1, C_2 and C_3, respectively. As shown in Fig. 1, each atom possesses one excited state $|e\rangle$ and three ground states $|g_l\rangle$, $|g_o\rangle$ and $|g_r\rangle$. The cavities C_1 and C_3 are single mode, and the cavity C_2 is bi-mode. C_1, C_2 and C_3 are connected by the optical fibers f_1, f_2, respectively. Assuming that the transition $|e\rangle_{a_{1(3)}} \leftrightarrow |g_o\rangle_{a_{1(3)}}$ is resonantly driven by a external classical field with the time-dependent Rabi frequency $\Omega_{1(3)}(t)$, while the transition $|e\rangle_{1(2)} \leftrightarrow |g_l\rangle_{1(2)}(|e\rangle_{2(3)} \leftrightarrow |g_r\rangle_{2(3)})$ is resonantly coupled to the left-circularly (right-circularly) polarized cavity mode with the coupling constant $g_{l(r)}$, respectively.

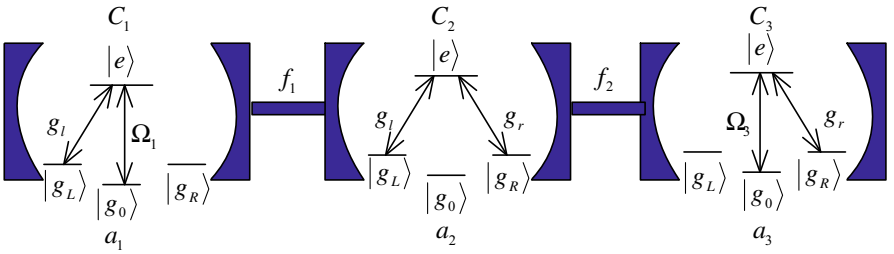

Fig. 1 The structure of the experimental setup and atoms. Three identical atoms a_1, a_2 and a_3 are trapped in three separated cavities C_1, C_2 and C_3, which are linked by two fibers f_1, f_2

In the short-fiber limit, i.e., $(2L\bar{\nu})/(2\pi c) \ll 1$ (L is the length of the fibers, $\bar{\nu}$ is the decay rate of the cavity fields into a continuum of fiber modes and c is the speed of light), only one resonant mode of the fiber interacts with the cavity mode [40]. In the rotating frame, the Hamiltonian of the whole system can be written as ($\hbar = 1$)

$$\begin{aligned} H_{\rm tot} &= H_l + H_c, \\ H_l &= \sum_{o=1,3} \Omega_o(t)|e\rangle_{a_o}\langle g_0| + H.c., \\ H_c &= g_{1l}a_{1l}|e\rangle_{a_1}\langle g_l| + g_{2l}a_{2l}|e\rangle_{a_2}\langle g_l| + g_{2r}a_{2r}|e\rangle_{a_2}\langle g_r| + g_{3r}a_{3r}|e\rangle_{a_3}\langle g_r| \\ &\quad + v_1 b_1^{\dagger}(a_{1l} + a_{2l}) + v_2 b_2^{\dagger}(a_{2r} + a_{3r}) + H.c., \end{aligned} \tag{7}$$

where $a_{kl}^{\dagger}$ ($a_{kr}^{\dagger}$) and a_{kl} (a_{kr}) denote the creation and annihilation operators for the left-circularly (right-circularly) polarized mode of cavities C_k ($k = 1,\ 2,\ 3$), respectively; $b_j^{\dagger}$ and b_j denote the creation and annihilation operators associated with the resonant mode of fiber f_j ($j = 1,\ 2$), respectively. For the sake of simplicity, we assume $g_{1l} = g_{2l} = g_{2r} = g_{3r} = g$ and $v_1 = v_2 = v$. If the initial state of the whole system is $|g_o g_l g_r\rangle|0\rangle_{C_1}|00\rangle_{C_2}|0\rangle_{C_3}|0\rangle_{f_1}|0\rangle_{f_2}$ (here $|g_o g_l g_r\rangle = |g_o g_l g_r\rangle_{a_1 a_2 a_3}$), the whole system evolves in the following subspaces

$$\begin{aligned} |\phi_1\rangle &= |g_o g_l g_r\rangle|0\rangle_{C_1}|00\rangle_{C_2}|0\rangle_{C_3}|0\rangle_{f_1}|0\rangle_{f_2}, & |\phi_2\rangle &= |e g_l g_r\rangle|0\rangle_{C_1}|00\rangle_{C_2}|0\rangle_{C_3}|0\rangle_{f_1}|0\rangle_{f_2}, \\ |\phi_3\rangle &= |g_l g_l g_r\rangle|1\rangle_{C_1}|00\rangle_{C_2}|0\rangle_{C_3}|0\rangle_{f_1}|0\rangle_{f_2}, & |\phi_4\rangle &= |g_l g_l g_r\rangle|0\rangle_{C_1}|00\rangle_{C_2}|0\rangle_{C_3}|1\rangle_{f_1}|0\rangle_{f_2}, \\ |\phi_5\rangle &= |g_l g_l g_r\rangle|0\rangle_{C_1}|10\rangle_{C_2}|0\rangle_{C_3}|0\rangle_{f_1}|0\rangle_{f_2}, & |\phi_6\rangle &= |g_l e g_r\rangle|0\rangle_{C_1}|00\rangle_{C_2}|0\rangle_{C_3}|0\rangle_{f_1}|0\rangle_{f_2}, \\ |\phi_7\rangle &= |g_l g_r g_r\rangle|0\rangle_{C_1}|01\rangle_{C_2}|0\rangle_{C_3}|0\rangle_{f_1}|0\rangle_{f_2}, & |\phi_8\rangle &= |g_l g_r g_r\rangle|0\rangle_{C_1}|00\rangle_{C_2}|0\rangle_{C_3}|0\rangle_{f_1}|1\rangle_{f_2}, \\ |\phi_9\rangle &= |g_l g_r g_r\rangle|0\rangle_{C_1}|00\rangle_{C_2}|1\rangle_{C_3}|0\rangle_{f_1}|0\rangle_{f_2}, & |\phi_{10}\rangle &= |g_l g_r e\rangle|0\rangle_{C_1}|00\rangle_{C_2}|0\rangle_{C_3}|0\rangle_{f_1}|0\rangle_{f_2}, \\ |\phi_{11}\rangle &= |g_l g_r g_o\rangle|0\rangle_{C_1}|00\rangle_{C_2}|0\rangle_{C_3}|0\rangle_{f_1}|0\rangle_{f_2}, \end{aligned} \tag{8}$$

where $|ijk\rangle$ ($i,\ j,\ k \in [e,\ g_l,\ g_o,\ g_r]$) denotes the state of the atoms in every cavity, $|n\rangle_s$ ($s = C_1,\ C_3,\ f_1,\ f_2$) means that the quantum field state of system contains n photons. $|n_1 n_2\rangle_{C_2}$ means that the number of left-circularly photon is n_1 and the number of right-circularly photon is n_2 in the cavity C_2.

Under the Zeno condition $g, v \gg \Omega_1, \Omega_3$, the Hilbert subspace is split into nine invariant Zeno subspace

$$
\begin{aligned}
&Z_1 = \{|\phi_1\rangle, |\psi_1\rangle, |\phi_{11}\rangle\}, \quad Z_2 = \{|\psi_2\rangle\}, \quad Z_3 = \{|\psi_3\rangle\} \\
&Z_4 = \{|\psi_4\rangle\}, \quad Z_5 = \{|\psi_5\rangle\}, \quad Z_6 = \{|\psi_6\rangle\}, \\
&Z_7 = \{|\psi_7\rangle\}, \quad Z_8 = \{|\psi_8\rangle\}, \quad Z_9 = \{|\psi_9\rangle\},
\end{aligned} \tag{9}
$$

where the eigenstates of H_c are

$$
\begin{aligned}
|\psi_1\rangle &= N_1(|\phi_2\rangle - \frac{g}{v}|\phi_4\rangle + |\phi_6\rangle - \frac{g}{v}|\phi_8\rangle + |\phi_{10}\rangle), \\
|\psi_2\rangle &= N_2(-|\phi_2\rangle + \varepsilon_1|\phi_3\rangle - \eta_1|\phi_4\rangle - \chi_1|\phi_5\rangle + \chi_1|\phi_7\rangle + \eta_1|\phi_8\rangle - \epsilon_1|\phi_9\rangle + |\phi_{10}\rangle), \\
|\psi_3\rangle &= N_3(-|\phi_2\rangle - \varepsilon_1|\phi_3\rangle - \eta_1|\phi_4\rangle + \chi_1|\phi_5\rangle - \chi_1|\phi_7\rangle + \eta_1|\phi_8\rangle + \epsilon_1|\phi_9\rangle + |\phi_{10}\rangle), \\
|\psi_4\rangle &= N_4(|\phi_2\rangle - \mu_1|\phi_3\rangle - \zeta_1|\phi_4\rangle + \delta_1|\phi_5\rangle - \theta_1|\phi_6\rangle + \delta_1|\phi_7\rangle - \zeta_1|\phi_8\rangle - \mu_1|\phi_9\rangle + |\phi_{10}\rangle), \\
|\psi_5\rangle &= N_5(|\phi_2\rangle + \mu_1|\phi_3\rangle - \zeta_1|\phi_4\rangle - \delta_1|\phi_5\rangle - \theta_1|\phi_6\rangle - \delta_1|\phi_7\rangle - \zeta_1|\phi_8\rangle + \mu_1|\phi_9\rangle + |\phi_{10}\rangle), \\
|\psi_6\rangle &= N_6(-|\phi_2\rangle + \varepsilon_2|\phi_3\rangle - \eta_2|\psi_4\rangle + \chi_2|\phi_5\rangle - \chi_2|\phi_7\rangle + \eta_2|\phi_8\rangle - \epsilon_2|\phi_9\rangle + |\phi_{10}\rangle), \\
|\psi_7\rangle &= N_7(-|\phi_2\rangle - \varepsilon_2|\phi_3\rangle - \eta_2|\psi_4\rangle - \chi_2|\phi_5\rangle + \chi_2|\phi_7\rangle + \eta_2|\phi_8\rangle + \epsilon_2|\phi_9\rangle + |\phi_{10}\rangle), \\
|\psi_8\rangle &= N_8(|\phi_2\rangle - \mu_2|\phi_3\rangle + \zeta_2|\phi_4\rangle - \delta_2|\phi_5\rangle + \theta_2|\phi_6\rangle - \delta_2|\phi_7\rangle + \zeta_2|\phi_8\rangle - \mu_2|\phi_9\rangle + |\phi_{10}\rangle), \\
|\psi_9\rangle &= N_9(|\phi_2\rangle + \mu_2|\phi_3\rangle + \zeta_2|\phi_4\rangle + \delta_2|\phi_5\rangle + \theta_2|\phi_6\rangle + \delta_2|\phi_7\rangle + \zeta_2|\phi_8\rangle + \mu_2|\phi_9\rangle + |\phi_{10}\rangle),
\end{aligned} \tag{10}
$$

with the corresponding eigenvalues

$$
\begin{aligned}
&\lambda_1 = 0, \quad \lambda_2 = -\sqrt{(g^2 + 2v^2 - A)/2}, \quad \lambda_3 = \sqrt{(g^2 + 2v^2 - A)/2}, \\
&\lambda_4 = -\sqrt{(3g^2 + 2v^2 - A)/2}, \quad \lambda_5 = \sqrt{(3g^2 + 2v^2 - A)/2}, \quad \lambda_6 = -\sqrt{(g^2 + 2v^2 + A)/2}, \\
&\lambda_7 = \sqrt{(g^2 + 2v^2 + A)/2}, \quad \lambda_8 = -\sqrt{(3g^2 + 2v^2 + A)/2}, \quad \lambda_9 = \sqrt{(3g^2 + 2v^2 + A)/2},
\end{aligned} \tag{11}
$$

where the parameters are

$$
\begin{aligned}
&\epsilon_1 = \frac{\sqrt{g^2 + 2v^2 - A}}{\sqrt{2}g}, \quad \eta_1 = \frac{-g^2 + 2v^2 - A}{2gv}, \quad \chi_1 = \frac{\sqrt{g^2 + 2v^2 - A}(g^2 + A)}{2\sqrt{2}gv^2}, \\
&\mu_1 = \frac{\sqrt{3g^2 + 2v^2 - A}}{\sqrt{2}g}, \quad \zeta_1 = \frac{-g^2 - 2v^2 + A}{2gv}, \quad \delta_1 = \frac{\sqrt{3g^2 + 2v^2 - A}(-g^2 + A)}{2\sqrt{2}gv^2}, \\
&\theta_1 = \frac{-g^2 + A}{v^2}, \quad \epsilon_2 = \frac{\sqrt{g^2 + 2v^2 + A}}{\sqrt{2}g}, \quad \eta_2 = \frac{-g^2 + 2v^2 + A}{2gv}, \\
&\chi_2 = \frac{\sqrt{g^2 + 2v^2 + A}(-g^2 + A)}{2\sqrt{2}gv^2}, \quad \mu_2 = \frac{\sqrt{3g^2 + 2v^2 + A}}{\sqrt{2}g}, \quad \zeta_2 = \frac{g^2 + 2v^2 + A}{2gv}, \\
&\delta_2 = \frac{\sqrt{3g^2 + 2v^2 + A}(g^2 + A)}{2\sqrt{2}gv^2}, \quad \theta_2 = \frac{g^2 + A}{v^2},
\end{aligned} \tag{12}
$$

in addition, $A = \sqrt{g^4 + 4v^4}$ and N_w is the normalization factor of the eigenstate $|\psi_w\rangle$ $(w = 1, 2, \ldots, 9)$.

The projector in the kth Zeno subspace Z_k is

$$
P_k^{\beta} = |\beta\rangle\langle\beta|, \quad (|\beta\rangle \in Z_k). \tag{13}
$$

The Hamiltonian in Eq. (8) can be approximately given by

$$H_{\rm tot} \simeq \sum_{k,\beta,\gamma} \lambda_k P_k^{\beta} + P_k^{\beta} H_l P_k^{\gamma}$$
$$= \sum_{k=2}^{9} \lambda_k |\psi_k\rangle\langle\psi_k| + N_1(\Omega_1|\phi_1\rangle\langle\psi_1| + \Omega_3|\phi_{11}\rangle\langle\psi_1| + H.c.). \quad (14)$$

If the initial state is $|g_o g_l g_r\rangle|0\rangle_{C_1}|00\rangle_{C_2}|0\rangle_{C_3}|0\rangle_{f_1}|0\rangle_{f_2}$, it reduces to

$$H_{eff} = N_1(\Omega_1|\phi_1\rangle\langle\psi_1| + \Omega_3|\phi_{11}\rangle\langle\psi_1| + H.c.), \quad (15)$$

which can be treated as a simple three-level system with an excited state $|\psi_1\rangle$ and two ground states $|\phi_1\rangle$ and $|\phi_{11}\rangle$. Then we obtain the eigenvectors and eigenvalues of the effective Hamiltonian $H_{\rm eff}$ as

$$|\eta_o(t)\rangle = \begin{pmatrix} \cos\theta(t) \\ 0 \\ -\sin\theta(t) \end{pmatrix}, \quad |\eta_\pm(t)\rangle = \frac{1}{\sqrt{2}} \begin{pmatrix} \sin\theta(t) \\ \pm 1 \\ \cos\theta(t) \end{pmatrix}, \quad (16)$$

with the corresponding eigenvalues $\eta_0 = 0$ and $\eta_\pm = \pm N_1\Omega$, and $\tan\theta = \frac{\Omega_1}{\Omega_3}$ and $\Omega = \sqrt{\Omega_1^2 + \Omega_3^2}$.

4 The generation of the three-atom GHZ state via transitionless quantum driving and adiabatic passage

4.1 Adiabatic passage method

For the sake of the clearness, we first briefly present how to generate the three-atom GHZ state via adiabatic passage. When the adiabatic condition $|\langle n_0|\partial_t n_\pm\rangle| \ll |\lambda'_\pm|$ is fulfilled well and the initial state is $|\psi(0)\rangle = |\phi_1\rangle$, the state evolution will always follow $|n_0(t)\rangle$ closely. To generate the three-atom GHZ state via the adiabatic passage and meet the boundary conditions of the fractional stimulated Raman adiabatic passage (STIRAP),

$$\lim_{t\to-\infty} \frac{\Omega_1(t)}{\Omega_3(t)} = 0, \quad \lim_{t\to+\infty} \frac{\Omega_3(t)}{\Omega_1(t)} = \tan\alpha, \quad (17)$$

we need properly to tailor the Rabi frequencies $\Omega_1(t)$ and $\Omega_3(t)$ in the original Hamiltonian $H_{\rm tot}$

$$\Omega_1(t) = \sin\alpha\Omega_0 \exp\left[\frac{-(t - t_0 - t_f/2)^2}{t_c^2}\right],$$
$$\Omega_3(t) = \Omega_0 \exp\left[\frac{-(t + t_0 - t_f/2)^2}{t_c^2}\right] + \cos\alpha\Omega_0 \exp\left[\frac{-(t - t_0 - t_f/2)^2}{t_c^2}\right], \quad (18)$$

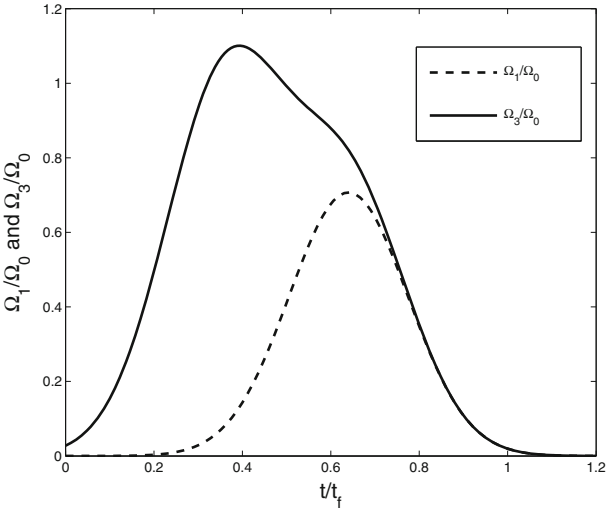

Fig. 2 The laser pulses Ω_1/Ω_0 and Ω_3/Ω_0 versus t/t_f

where Ω_0 is the pulse amplitude and t_f is the operation time. t_c and t_0 are some related parameters to be chosen for the best performance of the adiabatic passage process. In order to achieve better performance and meet the boundary conditions, we suitably chose the parameters that $\tan\alpha = 1$, $t_0 = 0.14t_f$ and $t_c = 0.19t_f$. As shown in Fig. 2, the time-dependent $\Omega_1(t)/\Omega_0$ and $\Omega_3(t)/\Omega_0$ versus t/t_f are plotted with the fixed values t_0 and t_c. With the above parameters, we obtain our wanted three-atom GHZ state $|\psi(t_f)\rangle = (|\phi_1\rangle - |\phi_{11}\rangle)/\sqrt{2}$ via the adiabatic passage. But this evolution process needs a relatively long time to satisfy the adiabatic condition. We will detail the reasons in the section of numerical simulations and analyses.

4.2 Transitionless quantum driving method

To reduce the evolution time and obtain the same state as the adiabatic passage, we use the approach of TQD to construct STAP. As introduced in the above, STAP speeds up a slow adiabatic passage via a non-adiabatic passage route to achieve a same outcome, and the TQD method is a important route to construct shortcuts. According to the ideas proposed by Berry [31], the instantaneous states in Eq. (16) do not meet the Schrödinger equation, i.e., $i\partial_t|n_k\rangle \neq H_{eff}|n_k\rangle (k = 0, \pm)$, so the situation that the system starts from the state $|\psi_n(0)\rangle$ and ends up in the state $|\psi_{m\neq n}(t)\rangle$ occurs in a finite probability even under the adiabatic condition. To drive the instantaneous states $|n_k\rangle (k = 0, \pm)$ exactly, we look for a Hamiltonian $H(t)$ related to the original Hamiltonian H_{eff} according to Berry's transitionless tracking algorithm [31]. From Sect. 2, we know the simplest Hamiltonian $H(t)$ possessed the form,

$$H(t) = i\sum_{0,\pm} |\partial_t n_k(t)\rangle\langle n_k(t)|. \tag{19}$$

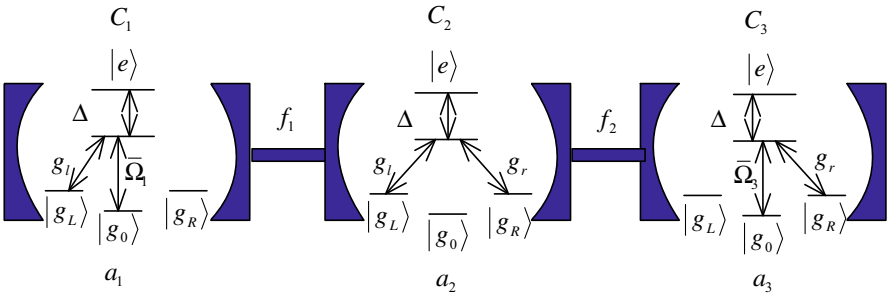

Fig. 3 The structure of the experimental setup and atoms for the APF Hamiltonian

Substituting Eq. (16) in Eq. (19), we obtain

$$H(t) = i\dot{\theta}|\phi_1\rangle\langle\phi_{11}| + H.c., \tag{20}$$

where $\dot{\theta} = [\dot{\Omega}_1(t)\Omega_3(t) - \Omega_1(t)\dot{\Omega}_3(t)]/\,\Omega^2$. This is our wanted CCD Hamiltonian to construct STAP, and we will detail how to construct this Hamiltonian in experiment later.

For the present system, the CDD Hamiltonian $H(t)$ is given in Eq. (18), but it is irrealizable under current experimental condition. Inspired by Refs. [18,20], we find an alternative physically feasible (APF) Hamiltonian whose effect is equivalent to $H(t)$. The design is shown in Fig. 3; the atomic transitions are not resonantly coupled to the classical lasers and cavity modes with the detuning Δ. The Hamiltonian of the system reads $H'_{\text{tot}} = H_c + H_l + H_d$, where $H_d = \sum_{k=1}^{3} \Delta|e\rangle_k\langle e|$. Then, similar to the approximation by QZD in Sect. 3, we also obtain an effective Hamiltonian for the non-resonant system

$$H'_{\text{eff}} = N_1(\overline{\Omega}_1|\phi_1\rangle\langle\psi_1| + \overline{\Omega}_3|\phi_{11}\rangle\langle\psi_1| + H.c.) + 3\Delta N_1^2|\psi_1\rangle\langle\psi_1|. \tag{21}$$

When the large detuning condition $3\Delta N_1 \geq \overline{\Omega}_1,\ \overline{\Omega}_3$ is satisfied, we can adiabatically eliminate the state $|\psi_1\rangle$ and obtain the final effective Hamiltonian

$$H_{\text{fe}} = -\frac{\overline{\Omega}_1^2}{3\Delta}|\phi_1\rangle\langle\phi_1| - \frac{\overline{\Omega}_3^2}{3\Delta}|\phi_{11}\rangle\langle\phi_{11}| - \frac{\overline{\Omega}_1\overline{\Omega}_3}{3\Delta}(|\phi_1\rangle\langle\phi_{11}| + |\phi_{11}\rangle\langle\phi_1|). \tag{22}$$

For simplicity, we set $\overline{\Omega}_1 = \overline{\Omega}_3 = \overline{\Omega}(t)$. The front two terms caused by Stark shift can be removed and the Hamiltonian becomes

$$\overline{H}(t) = \Omega_x|\phi_1\rangle\langle\phi_{11}| + H.c., \tag{23}$$

where $\Omega_x = -\frac{\overline{\Omega}^2}{3\Delta}$. The equation has a similar form with Eq. (20), but the effective couplings between $i\dot{\theta}$ and Ω_x exist $3\pi/2$-dephased. To guarantee their consistency, we put a change that $\Omega_3 \to -i\Omega_3$. Then, the eigenstates of H_{eff} become

$$|\eta_o'(t)\rangle = \begin{pmatrix} \cos\theta(t) \\ 0 \\ i\sin\theta(t) \end{pmatrix}, \quad |\eta_\pm'(t)\rangle = \frac{1}{\sqrt{2}} \begin{pmatrix} \sin\theta(t) \\ \pm 1 \\ -i\cos\theta(t) \end{pmatrix}, \tag{24}$$

and the CDD Hamiltonian $H(t)$ becomes

$$H(t) = -\dot{\theta}|\phi_1\rangle\langle\phi_{11}| - \dot{\theta}|\phi_{11}\rangle\langle\phi_1|. \tag{25}$$

Compared Eq. (23) with Eq. (25), we can easily get the CDD Hamiltonian when the condition $\Omega_x = -\dot{\theta}$ is satisfied.

$$\overline{\Omega}_1(t) = \overline{\Omega}_3(t) = \overline{\Omega}(t) = \sqrt{3\Delta\dot{\theta}}. \tag{26}$$

4.3 Numerical simulations and analyses

Next we will show that it takes less time to get the target state on the situation governed by the APF Hamiltonian H'_{tot} via TQD than by the original Hamiltonian H_{tot} via adiabatic passage. The time-dependent population for any state $|\psi\rangle$ is defined as $P = |\langle\psi|\rho(t)|\psi\rangle|$, where $\rho(t)$ is the corresponding time-dependent density operator. We present the fidelity versus the laser pulses amplitude Ω_o and the operation time t/t_f via adiabatic passage in Fig. 4. As shown in Fig. 4, we can know that the bigger the laser pulse amplitude is, the less time that the system evolution to the target state needs. However, the value of the Rabi frequencies needs to meet some conditions. Firstly, we need to satisfy the Zeno conditions $g, v \gg \Omega_1, \Omega_3$, so we set $\Omega_0 = 0.2g$; Secondly, it has to ensure that the rotating wave approximation is effective; the last,

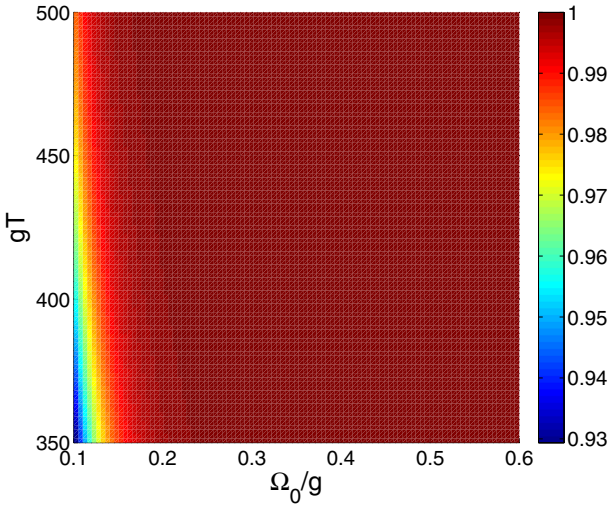

Fig. 4 The fidelity versus the laser pulses amplitude Ω_0 and the operation time t/t_f

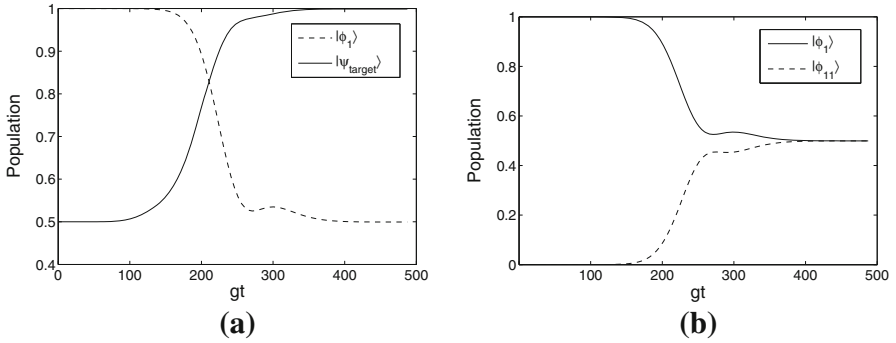

Fig. 5 **a** The population P_{target} of the target state $|\psi_{\text{target}}\rangle$ and the population P_0 of the initial state $|\psi(0)\rangle$ governed by the original Hamiltonian H_{tot} via the adiabatic passage. **b** The population $P_1(t)$ of the states $|\phi_1\rangle$ and the population $P_{11}(t)$ of the states $|\phi_{11}\rangle$ governed by the original Hamiltonian H_{tot} via adiabatic passage. The parameters are collectively with the fixed values $\Omega_0 = 0.2g$, $g = v$, $t_0 = 0.14t_f$, $t_c = 0.19t_f$ and $t_f = 400/g$

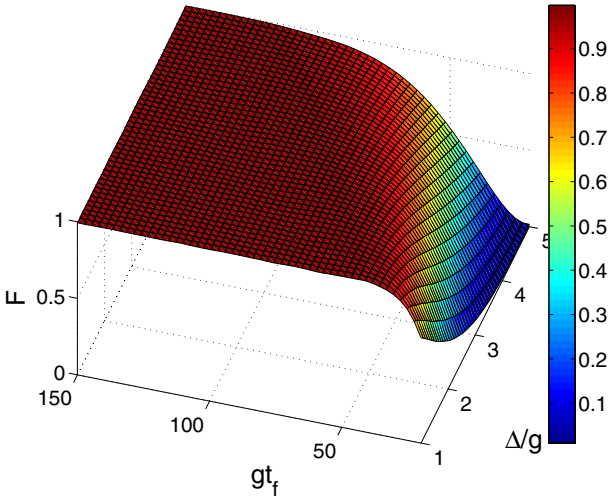

Fig. 6 The fidelity F of the target state $|\psi(t_f)\rangle$ governed by H'_{tot} versus the interaction time gt_f and the detuning Δ/g

it has to avoid to excite high-photon energy levels. In Fig. 5, we display the time-dependent populations of the states $|\phi_1\rangle$, $|\psi_{\text{target}}\rangle$, and $|\phi_{11}\rangle$ via adiabatic passage. As depicted in Figs. 4 and 5, the operation time needs $t_f \geq 400/g$ to achieve an ideal result at least. It is awkward in some case.

Next we will detail the evolution governed by the APF Hamiltonian H'_{tot} via TQD. According to Eq. (24), we finally get a GHZ state $|\psi(t_f)\rangle = \frac{1}{\sqrt{2}}(|\phi_1\rangle + i|\phi_{11}\rangle)$. In Fig. 6, we present the relationship between the fidelity of the three-atom GHZ state (governed by the APF Hamiltonian) and two parameters Δ and t_f when $\Omega_0 = 0.2g$ to satisfy the Zeno condition, where the fidelity of the three-atom GHZ state is defined as $F = |\langle \text{GHZ}|\rho(t_f)|\text{GHZ}\rangle|$ ($\rho(t_f)$ is the density operator of the whole system when

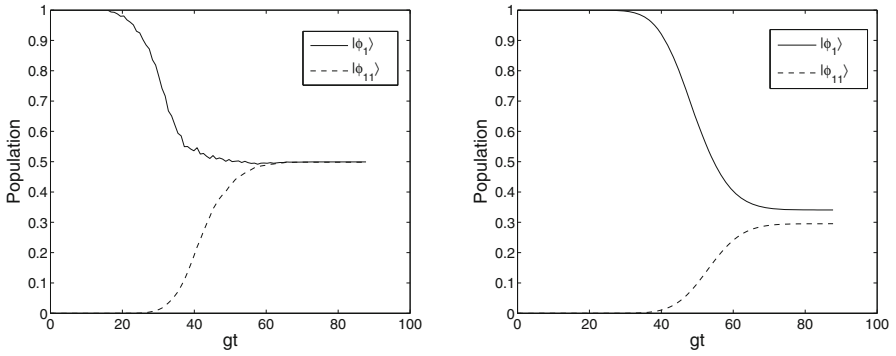

Fig. 7 The population $P_1(t)$ of the state $|\phi_1\rangle$ and the population $P_{11}(t)$ of the state $|\phi_{11}\rangle$ governed by **a** the APF Hamiltonian $H'_{\rm tot}$ with $\Delta = 2.3g$. **b** The original Hamiltonian $H_{\rm tot}$ collectively with the fixed values $\Omega_0 = 0.2g$, $g = v$, $t_0 = 0.14t_f$, $t_c = 0.19t_f$, and $t_f = 72/g$

$t = t_f$). We find that a wide range for parameters Δ and t_f can obtain a high fidelity of the three-atom GHZ state, and the fidelity increases with the increasing of Δ and the decreasing of t_f. In order to satisfy the large detuning condition, we set $\Delta = 2.3g$. Figure 6 reveals that the operation time needs $t_f \geq 72/g$ via TQD at least. In Fig. 7, we plot the operation time for the creation of the GHZ state governed by $H'_{\rm tot}$ and by $H_{\rm tot}$ with the parameters that $t_f = 72/g$, $\Omega_0 = 0.2g$, $\Delta = 2.3g$ and $g = v$. Numerical results show that the APF Hamiltonian $H'_{\rm tot}$ can govern the evolution to a perfect GHZ state $|\psi(t_f)\rangle$ from $|\psi_1\rangle$ in a relatively short interaction time while the original Hamiltonian $H_{\rm tot}$ cannot.

In above analysis, we do not consider the influence of decoherence caused by various factors, such as spontaneous emissions, cavity decays and fiber photon leakages. In fact, the decoherence is unavoidable during the evolution of the whole system in experiment. The master equation of the whole system is written as

$$\begin{aligned}\dot{\rho} = &-i[H_{\rm tot}, \rho] \\ &+ \sum_{k=1}^{3} \frac{\gamma_k}{2} \left(2\sigma_k^- \rho \sigma_k^+ - \sigma_k^+ \sigma_k^- \rho - \rho \sigma_k^+ \sigma_k^-\right) \\ &+ \sum_{k=1}^{2} \frac{\kappa_{c_k}}{2} \left(2a_{l,k} \rho a_{l,k}^+ - a_{l,k}^+ a_{l,k} \rho - \rho a_{l,k}^+ a_{l,k}\right) \\ &+ \sum_{k=2}^{3} \frac{\kappa_{c_k}}{2} \left(2a_{r,k} \rho a_{r,k}^+ - a_{r,k}^+ a_{r,k} \rho - \rho a_{r,k}^+ a_{r,k}\right) \\ &+ \sum_{k=1}^{2} \frac{\kappa_{f_k}}{2} \left(2b_k \rho b_k^+ - b_k^+ b_k \rho - \rho b_k^+ b_k\right), \end{aligned} \tag{27}$$

where γ_k is the atomic spontaneous emission rate for the kth atom and $\kappa_{c(f)}$ is the decay rate of the kth cavity (kth fiber), σ_k^- denotes the atomic transition from the ground

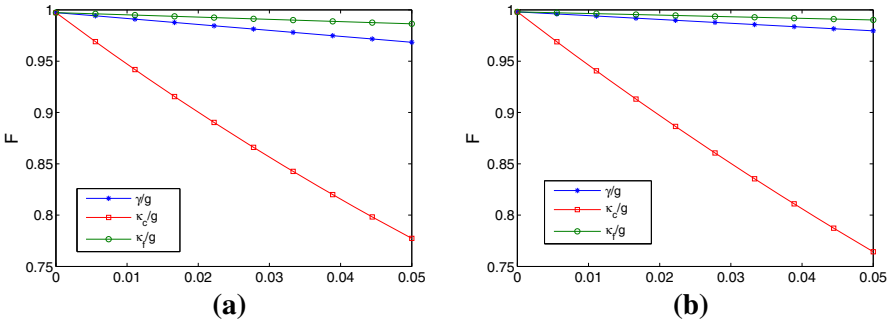

Fig. 8 The fidelity of the target state $|\psi(t_f)\rangle$ governed by **a** the APF Hamiltonian H'_{tot} with $\Delta = 2.3g$, $t_f = 72/g$ and $\Omega_0 = 0.2g$. **b** The original Hamiltonian H_{tot} with $t_f = 153/g$, and $\Omega_0 = 0.5g$ collectively with the fixed values $t_0 = 0.14t_f$, and $t_c = 0.19t_f$ versus the dimensionless parameters γ/g, κ_c/g, and κ_f/g, respectively

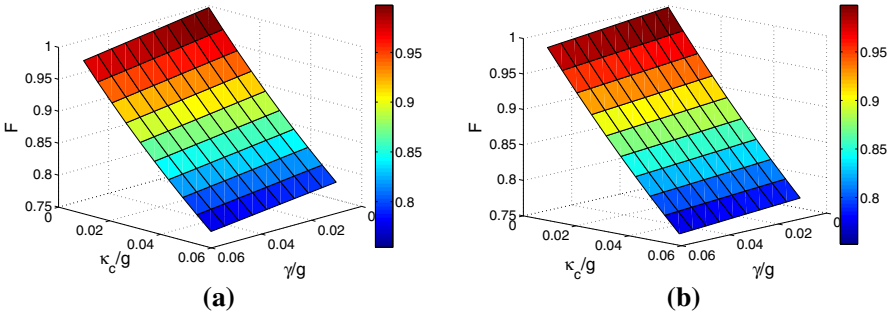

Fig. 9 The fidelity of the target state $|\psi(t_f)\rangle$ governed by **a** the APF Hamiltonian H'_{tot} with $\Delta = 2.3g$, $t_f = 72/g$, and $\Omega_0 = 0.2g$. **b** The original Hamiltonian H_{tot} with $t_f = 153/g$, and $\Omega_0 = 0.5g$ collectively with the fixed values $t_0 = 0.14t_f$, and $t_c = 0.19t_f$ versus the dimensionless parameters γ/g and κ_c/g

states $|m\rangle$ $(m = g_0,\ g_l,\ g_r)$ to the excited state $|e\rangle$. For the sake of simplicity, we assume that $\gamma_1 = \gamma_2 = \gamma_3 = \gamma, \kappa_{c_1} = \kappa_{c_2} = \kappa_{c_3} = \kappa_c$ and $\kappa_{f_1} = \kappa_{f_2} = \kappa_f$. As shown in Fig. 8, we plot the fidelity governed by the APF Hamiltonian H'_{tot} and by the original Hamiltonian H_{tot} and the dimensionless parameters $\gamma/g, \kappa_c/g$ and κ_f/g, respectively. We can draw a conclusion that the fidelities are almost unaffected by the fiber decay both via TQD and via adiabatic passage. We focus on the main decoherence factors included the cavity decay and the atomic spontaneous emission. As shown in Fig. 9, we plot the fidelity versus the cavity decay and the atomic spontaneous emission. We can know the most important decoherence factor is the cavity decay. This result can be understood from Ref. [19] that if the Zeno condition cannot be satisfied very well, the populations of the intermediate states including the cavity excited states cannot be suppressed ideally.

From the above analyses, we can obviously know that the evolution time from the initial state to the target state via TQD is $t_f = 72/g$ when $\Omega_0 = 0.2g$, $\Delta = 2.3g$, $t_0 = 0.14t_f, t_c = 0.19t_f$ and $g = v$, while the evolution time for the adiabatic passage is $t_f = 400/g$ when $\Omega_0 = 0.2g$, $t_0 = 0.14t_f$, $t_c = 0.19t_f$ and $g = v$. So, the benefit of the TQD method is shown obviously that the speed via TQD method is faster than

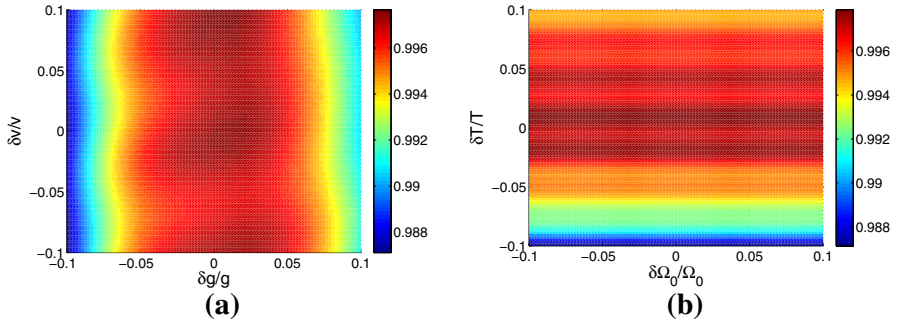

Fig. 10 The fidelity of the target state $|\psi_{\text{target}}\rangle$ versus the deviations of **a** g and v, **b** T and Ω_0

that via adiabatic passage. It is more worthy to note that the fidelity of the target state via TQD is almost equal to that via adiabatic passage. So our scheme has a huge advantage compared with the proposals via adiabatic passage. That means the present scheme via STAP method is not only fast but also robust.

As we all know, it is necessary for a good scheme to tolerate the deviations of the experimental parameters, because it is impossible to avoid the operational imperfection in experiment. Define that $\delta x = x' - x$ is the deviation of the ideal value x, x' is the actual value. In Fig. 10, we plot the fidelity of the target state $|\psi_{\text{target}}\rangle$ versus the deviations of the experimental parameters g, v, Ω_0, and T ($T = t_f$ denotes the operation time). Numerical results demonstrate that our scheme is robust against the fluctuation of the experimental parameters.

5 The generation of the N-atom GHZ state via transitionless quantum driving

Next we briefly present the generalization of the scheme in Sect. 4 to generate N-atom GHZ state by the same principle. We consider the physical configuration shown in Fig. 11, where N atoms $a_1,\ a_2, \ldots, a_N$ are trapped in N cavities $C_1,\ C_2, \ldots, C_N$ connected by $N-1$ fibers $f_1,\ f_2, \ldots, f_{N-1}$, respectively. The level configurations of the atoms between two ends are the same as that of the atom a_2 in the three-atom case, and the level configurations of a_1 and a_N are the same as those of a_1 and a_3 in the three-atom case, respectively. The Hamiltonian of the present system can be written as in the rotation framework

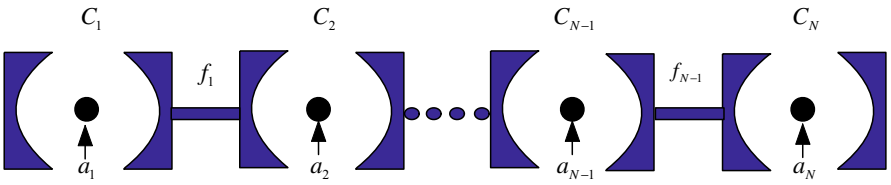

Fig. 11 The set-up diagram for the generation of N-atom GHZ states. The N-atoms are respectively trapped in N-cavities which are linked by $N-1$ fibers

$$
\begin{aligned}
H_{\text{total}} &= H_l' + H_c', \\
H_l' &= \Omega_1' |e\rangle_{a_1}\langle g_0| + \Omega_N' |e\rangle_{a_N}\langle g_0| + H.c., \\
H_c' &= \sum_{i=1}^{N-1} g_{i,l} a_{i,l} |e\rangle_{a_i}\langle g_l| + \sum_{j=2}^{N} g_{j,r} a_{j,r} |e\rangle_{a_j}\langle g_r| \\
&\quad + \sum_{k=2}^{N-1} [v_{k-1} b_{k-1}^{\dagger}(a_{k-1,l} + a_{k,l}) + v_k b_k^{\dagger}(a_{k,r} + a_{k+1,r})] + H.c..
\end{aligned} \tag{28}
$$

Let us consider the situation where N is an odd number, i.e., $N = 2l + 1$, $(l = 1, 2, 3, \ldots)$. Suppose that the initial state of the atoms is $|g_0 g_l g_r g_l g_r \ \ldots \ g_r\rangle$ while all the cavities and fibers are vacuum, then the system can be expended in the following subspace

$$
\begin{aligned}
&|\phi_1'\rangle = |g_0 g_l g_r \ \ldots \ g_r\rangle|0\rangle_{\text{all}}, \quad |\phi_2'\rangle = |e g_l g_r \ \ldots \ g_r\rangle|0\rangle_{\text{all}}, \\
&|\phi_3'\rangle = |g_l g_l g_r \ \ldots \ g_r\rangle|1\rangle_{c_1}, \quad |\phi_4'\rangle = |g_l g_l g_r \ \ldots \ g_r\rangle|1\rangle_{f_1}, \\
&|\phi_5'\rangle = |g_l g_l g_r \ \ldots \ g_r\rangle|10\rangle_{c_2}, \quad |\phi_6'\rangle = |g_l e g_r \ \ldots \ g_r\rangle|0\rangle_{\text{all}}, \\
&|\phi_7'\rangle = |g_l g_r g_r \ \ldots \ g_r\rangle|01\rangle_{c_2}, \quad |\phi_8'\rangle = |g_l g_r g_r \ \ldots \ g_r\rangle|1\rangle_{f_2}, \\
&|\phi_9'\rangle = |g_l g_r g_r \ \ldots \ g_r\rangle|01\rangle_{c_3}, \quad |\phi_{10}'\rangle = |g_l g_r e \ \ldots \ g_r\rangle|0\rangle_{\text{all}}, \ldots \\
&|\phi_{4N-1}'\rangle = |g_l g_r \ \ldots \ g_r g_0\rangle|0\rangle_{\text{all}},
\end{aligned} \tag{29}
$$

where $|0\rangle_{\text{all}}$ means that there is none photon in all boson modes, $|n_1 n_2\rangle_{s_i}$ $(s = C,\ f.i = 1, 2, \ldots, N)$ means that there are n_1 left-circularly photon and n_2 right-circularly photon in the corresponding cavity C_i or fiber f_i.

Similar to the above procedure from Eq. (10) to Eq. (16), we get an effective Hamiltonian

$$
H_{eff(N)} = N_1'(\Omega_1' |\phi_1'\rangle\langle\psi_1'| + \Omega_N' |\phi_{4N-1}'\rangle\langle\psi_1'| + H.c.), \tag{30}
$$

where

$$
|\psi_1'\rangle = N_1' \left(\sum_{i=1}^{N} |\phi_{4i-2}'\rangle - \sum_{i=1}^{N-1} \frac{g}{v} |\phi_{4i}'\rangle \right). \tag{31}
$$

In addition, the eigenstates and eigenvalues of the Hamiltonian in Eq. (30) can be written as

$$
|\chi_o(t)\rangle = \begin{pmatrix} \cos\theta'(t) \\ 0 \\ -\sin\theta'(t) \end{pmatrix}, \quad |\chi_{\pm}(t)\rangle = \frac{1}{\sqrt{2}} \begin{pmatrix} \sin\theta'(t) \\ \pm 1 \\ \cos\theta'(t) \end{pmatrix}, \tag{32}
$$

with the corresponding eigenvalues $\chi_0' = 0$ and $\chi_{\pm}' = \pm N_1' \Omega'$, where $\tan\theta' = \frac{\Omega_1'}{\Omega_N'}$ and $\Omega' = \sqrt{\Omega_1'^2 + \Omega_N'^2}$. Substituting Eq. (32) in Eq. (19), we obtain

$$H'(t) = i\dot{\theta}'|\phi'_1\rangle\langle\phi'_{4N-1}| + H.c., \tag{33}$$

where $\dot{\theta}' = [\dot{\Omega}'_1(t)\Omega'_N(t) - \Omega'_1(t)\dot{\Omega}'_N(t)]/\Omega'^2$.

Inspired by the above idea in Sect. 4, we make the system into a non-resonant system to construct the CDD Hamiltonian in Eq. (33). Therefore, the Hamiltonian of the present system reads $H'_{\text{total}} = H'_l + H'_c + H'_d$, where $H'_d = \sum_{i=1}^{N} \Delta|e\rangle\langle e|$. Similar to the above procedure from Eq. (22) to Eq. (23) in Sect. 4, we obtain the final effective Hamiltonian

$$\begin{aligned} H'_{fe(N)} = &-\frac{\overline{\Omega}'^2_1}{3\Delta}|\phi'_1\rangle\langle\phi'_1| - \frac{\overline{\Omega}'^2_N}{3\Delta}|\phi'_{4N-1}\rangle\langle\phi'_{4N-1}| \\ &- \frac{\overline{\Omega}'_1\overline{\Omega}'_N}{3\Delta}\left(|\phi'_1\rangle\langle\phi'_{4N-1}| + |\phi'_{4N-1}|\rangle\langle\phi'_1|\right). \end{aligned} \tag{34}$$

For simplicity, we set $\overline{\Omega}'_1 = \overline{\Omega}'_N = \overline{\Omega}'$, the front two terms caused by Stark shift can be omitted and the Hamiltonian becomes

$$\overline{H}_N = \Omega'_x(t)|\phi'_1\rangle\langle\phi'_{4N-1}| + H.c., \tag{35}$$

where $\Omega'_x(t) = -\frac{\overline{\Omega}'^2}{3\Delta}$. To guarantee their consistency, we put a change that $\Omega_N \to -i\Omega_N$. Then the eigenstates of $H_{\text{eff}(N)}$ become

$$|\chi'_o(t)\rangle = \begin{pmatrix} \cos\theta'(t) \\ 0 \\ i\sin\theta'(t) \end{pmatrix}, \quad |\chi'_{\pm}(t)\rangle = \frac{1}{\sqrt{2}}\begin{pmatrix} \sin\theta'(t) \\ \pm 1 \\ -i\cos\theta'(t) \end{pmatrix}, \tag{36}$$

and the CDD Hamiltonian $H(t)$ becomes

$$H'(t) = -\dot{\theta}'|\phi'_1\rangle\langle\phi'_{4N-1}| - \dot{\theta}'|\phi'_{4N-1}\rangle\langle\phi'_1|. \tag{37}$$

Compared Eq. (35) with Eq. (37), we can easily get the CDD Hamiltonian when the condition $\Omega'_x = -\dot{\theta}'$ is satisfied.

$$\overline{\Omega}'_1(t) = \overline{\Omega}'_N(t) = \overline{\Omega}'(t) = \sqrt{3\Delta\dot{\theta}'}. \tag{38}$$

6 Experimental feasibility and conclusions

Now experimental feasibility needs to be discussed. The configuration of ^{87}Rb can be suitable for our proposals. Under current experimental condition, a set of CQED parameters $g = 2\pi \times 750\,\text{MHz}$, $\gamma = 2\pi \times 2.62\,\text{MHz}$, and $\kappa_c = 2\pi \times 3.5\,\text{MHz}$ is available with the wavelength in the region 630–850 nm [41]. By using fiber-taper coupling to high-Q silica microspheres, the efficiency of fiber–cavity coupling is higher than 99.9 % [42]. The optical fiber decay at a 852 nm wavelength is about 2.2 dB/km

[43], which means the fiber decay rate is about $\kappa_f = 1.52 \times 10^5$ Hz. With the above parameters, we obtain a relatively high fidelity about 97.15 %.

In conclusion, we have proposed an efficient scheme to fast deterministically generate N-atom GHZ state in separate coupled cavities via transitionless quantum driving (TQD) only by one-step manipulation. We apply a promising method to construct STAP by joint utilization of the Zeno dynamics and the approach of TQD in the cavities QED system. The method features are that we do not need to control the time exactly and the evolution process is fast. Because the atoms are trapped in separate coupled cavity, the single-qubit manipulation can be realized easily. When considering dissipation, we can see that the method is robust against the decoherences caused by the atomic spontaneous emission and fiber decay. The results show that the scheme has a high fidelity and may be possible to implement with the current experimental technology. So, the scheme is fast, robust and effective. We hope the scheme can be used to generate multiatom GHZ state in the future.

Acknowledgments This work was supported by the National Natural Science Foundation of China under Grants Nos. 11105030 and 11374054, the Foundation of Ministry of Education of China under Grant No. 212085, and the Major State Basic Research Development Program of China under Grant No. 2012CB921601.

References

1. Zheng, S.B., Guo, G.C.: Efficient scheme for two-atom entanglement and quantum information processing in cavity QED. Phys. Rev. Lett. **85**, 2392 (2000)
2. Jia, X.J., Yan, Z.H., Duan, Z.Y., Su, X.L., Wang, H., Xie, C.D., Peng, K.C.: Experimental realization of three-color entanglement at optical fiber communication and atomic storage wavelength. Phys. Rev. Lett. **109**, 253604 (2012)
3. Bell, J.S.: On the Einstein–Podolsky–Rosen paradox. Physics **1**, 195 (1965)
4. Qin, Z.Z., Cao, L.M., Wang, H.L., Marino, A.M., Zhang, W.P., Jing, J.T.: Experimental generation of multiple quantum correlated beams from hot rubidium vapor. Phys. Rev. Lett. **113**, 023602 (2014)
5. Nielsen, M.A., Chuang, I.L.: Quantum Computation and Quantum Information. Cambridge University Press, Cambridge (2000)
6. Ekert, A.K.: Quantum cryptography based on Bell's theorem. Phys. Rev. Lett. **67**, 661 (1991)
7. Xia, Y., Song, J., Lu, P.M., Song, H.S.: Teleportation of an N-photon Greenberger–Horne–Zeilinger (GHZ) polarization entangled state using linear optical elements. J. Opt. Soc. Am. B **27**, A1 (2010)
8. Bennett, C.H., Brassard, G., Crepeau, C., Jozsa, R., Peres, A., Wootters, W.: Teleporting an unknown quantum state via dual classical and Einstein–Podolsky–Rosen channels. Phys. Rev. Lett. **70**, 1895 (1993)
9. Hillery, M., Buzek, V., Berthiaume, A.: Quantum secret sharing. Phys. Rev. A **59**, 1829 (1999)
10. Greenberger, D.M., Horne, M.A., Zeilinger, A.: Going beyond Bell's theorem. In: Kafators, M. (ed.) Bell's Theorem, Quantum Theory, and Conception of the Universe. Kluwer, Dordrecht (1989)
11. Greenberger, D.M., Horne, M.A., Shimony, A., Zeilinger, A.: Bell's theorem without inequalities. Am. J. Phys **58**, 1131 (1990)
12. Zheng, S.B.: Generation of Greenberger–Horne–Zeilinger states for multiple atoms trapped in separated cavities. Eur. Phys. J. D **54**, 719 (2009)
13. Zheng, S.B.: One-step synthesis multiatom Greenberger–Horne–Zeilinger states. Phys. Rev. Lett. **87**, 230404 (2001)
14. Leibfried, D., Knill, E., Seidelin, S., Britton, J., Blakestad, R.B., Chiaverini, J., Hume, D.B., Itano, W.M., Jost, J.D., Langer, C., Ozeri, R., Reichle, R., Wineland, D.J.: Creation of a six-atom 'Schrödinger cat' state. Nature **438**, 639 (2005)
15. Zhao, Z., Chen, Y.A., Zhang, A.N., Yang, T., Briegel, H.J., Pan, J.W.: Experimental demonstration of five-photon entanglement and open-destination teleportation. Nature **430**, 54 (2004)

16. Su, X.L., Tan, A.H., Jia, X.J., Zhang, J., Xie, C.D., Peng, K.C.: Experimental preparation of quadripartite cluster and Greenberger–Horne–Zeilinger states for continuous variables. Phys. Rev. Lett. **98**, 070502 (2007)
17. Raimond, J.M., Brune, M., Haroche, S.: Manipulating quantum entanglement with atoms and photons in a cavity. Rev. Mod. Phys. **73**, 565 (2001)
18. Shi, Z.C., Xia, Y., Song, J., Song, H.S.: One-step implementation of the Fredkin gate via Zeno dynamics. Quantum. Inf. Comput. **12**, 0215 (2012)
19. Li, W.A., Wei, L.F.: Controllable entanglement preparations between atoms in spatially-separated cavities via Zeno dynamics. Opt. Express **20**, 13440 (2012)
20. Hao, S.Y., Xia, Y., Song, J., An, N.B.: One-step generation of multiatom Greenberger–Horne–Zeilinger states in separate cavities via adiabatic passage. J. Opt. Soc. Am. B **30**, 468 (2013)
21. Chen, Y.H., Xia, Y., Chen, Q.Q., Song, J.: Universally shortcuts to adiabatic passage for generation of Greenberger-Horne-Zeilinger states by transitionless quantum driving. arXiv:1411.6747v3 (2014)
22. Chen, X., Lizuain, I., Ruschhaupt, A., Guéry-Odelin, D., Muga, J.G.: Shortcuts to adiabatic passage in two- and three-level atoms. Phys. Rev. Lett. **105**, 123003 (2010)
23. Chen, X., Muga, J.G.: Engineering of fast population transfer in three-level systems. Phys. Rev. A **86**, 033405 (2012)
24. Chen, Y.H., Xia, Y., Chen, Q.Q., Song, J.: Efficient shortcuts to adiabatic passage for fast population transfer in multiparticle systems. Phys. Rev. A **89**, 033856 (2014)
25. Lu, M., Xia, Y., Shen, L.T., Song, J., An, N.B.: Shortcuts to adiabatic passage for population transfer and maximum entanglement creation between two atoms in a cavity. Phys. Rev. A **89**, 012326 (2014)
26. Lu, M., Xia, Y., Shen, L.T., Song, J.: An effective shortcut to adiabatic passage for fast quantum state transfer in a cavity quantum electronic dynamics system. Laser Phys. **24**, 105201 (2014)
27. Chen, Y.H., Xia, Y., Chen, Q.Q., Song, J.: Shortcuts to adiabatic passage for multiparticles in distant cavities: applications to fast and noise-resistant quantum population transfer, entangled states' preparation and transition. Laser Phys. Lett. **11**, 115201 (2014)
28. Chen, Y.H., Xia, Y., Chen, Q.Q., Song, J.: Fast and noise-resistant implementation of quantum phase gates and creation of quantum entangled states. Phys. Rev. A **91**, 012325 (2015)
29. Liang, Y., Wu, Q.C., Su, S.L., Ji, X., Zhang, S.: Shortcuts to adiabatic passage for multiqubit controlled gate. Phys. Rev. A **91**, 032304 (2015)
30. Lewis, H.R., Riesenfeld, W.B.: An exact quantum theory of the time-dependent harmonic oscillator and of a charged particle in a time-dependent electromagnetic field. J. Math. Phys. **10**, 1458 (1969)
31. Berry, M.V.: Transitionless quantum driving. J. Phys. A **42**, 365303 (2009)
32. Chen, X., Torrontegui, E., Muga, J.G.: Lewis–Riesenfeld invariants and transitionless quantum driving. Phys. Rev. A **83**, 062116 (2011)
33. von Neumann, J.: Die mathematische grundlagen der quantenmechanik. Springer, Berlin (1932)
34. Misra, B., Sudarshan, E.C.G.: The Zeno's paradox in quantum theory. J. Math. Phys. **18**, 756 (1977)
35. Facchi, P., Gorini, V., Marmo, G., Pascazio, S., Sudarshan, E.C.G.: Quantum Zeno dynamics. Phys. Lett. A **275**, 12 (2000)
36. Facchi, P., Pascazio, S., Scardicchio, A., Schulman, L.S.: Zeno dynamics yields ordinary constraints. Phys. Rev. A **65**, 012108 (2002)
37. Facchi, P., Pascazio, S.: Quantum Zeno subspaces. Phys. Rev. Lett. **89**, 080401 (2002)
38. Facchi, P., Marmo, G., Pascazio, S.: Quantum Zeno dynamics and quantum Zeno subspaces. J. Phys. Conf. Ser. **196**, 012017 (2009)
39. Yang, R.C., Li, G., Zhang, T.C.: Robust atomic entanglement in two coupled cavities via virtual excitations and quantum Zeno dynamics. Quantum Inf. Process. **12**, 493 (2012)
40. Serafini, A., Mancini, S., Bose, S.: Distributed quantum computation via optical fibers. Phys. Rev. Lett. **96**, 101503 (2006)
41. Spollane, S.M., Kippenberg, T.J., Vahala, K.J., Goh, K.W., Wilcut, E., Kimble, H.J.: Ultrahigh-Q toroidal microresonators for cavity quantum electrodynamics. Phys. Rev. A **71**, 013817 (2005)
42. Spollane, S.M., Kippenberg, T.J., Painter, O.J., Vahala, K.J.: Ideality in a fiber-taper-coupled microresonator system for application to cavity quantum electrodynamics. Phys. Rev. Lett. **91**, 043902 (2003)
43. Gordon, K.J., Fernandez, V., Townsend, P.D., Buller, G.S.: A short wavelength gigahertz clocked fiber optic quantum key distribution system. IEEE J. Quantum Electron. **40**, 900 (2004)